Novel Active-Matrix Micro-LED Display With External Compensation Featuring Fingerprint Recognition

Dong-Hwan Jeon, Won-Been Jeong, and Seung-Woo Lee, *Senior Member, IEEE*

***Abstract*— This letter proposes a novel active-matrix (AM) micro light-emitting diode (micro-LED) display architecture featuring fingerprint detection. A new pixel circuit comprising four transistors and one capacitor (4T1C) is proposed to compensate for threshold voltages externally. The proposed AM micro-LED display does not need any additional light sources and sensors because an LED itself can be used for photosensors. The proposed 4T1C pixel circuit can isolate the effects of LED photocurrents caused by ambient lights and large LED capacitance from detecting the threshold voltage via external circuits. The proposed AM pixel circuit with oxide thin film transistors was fabricated using oxide thin film transistor process. The charges caused by the LED photocurrents were accumulated for 16.7 ms. The final voltages measured after 16.7 ms were −5.02 V and −1.53 V under irradiance of 0.05 W/m^2 and 1.54 W/m^2, respectively. It is verified that the proposed micro-LED pixel circuit could distinguish incident lights reflected from ridges and valleys of a fingerprint.**

***Index Terms*— Displays, fingerprint recognition, light emitting diode, sensors.**

I. Introduction

RECENTLY, a micro light emitting diode (micro-LED) display has emerged as a next-generation display featuring fast response times, high resolution, high contrast ratio, and so on [1]–[3]. Because it is a self-luminous display, it is very similar to an active-matrix organic light emitting diode (AMOLED) display. Thus, the intensity of emitting light from a micro-LED can be adjusted by an active device such as a thin-film transistor (TFT). However, the variation of the threshold voltages (V_{TH}s) of driving TFTs are inevitable. Furthermore, the threshold voltages may change with operation times [4]–[6]. This would result in non-uniform luminance, which degrades perceived display image quality. There are two ways to compensate for V_{TH}: the internal and external compensation methods. In the internal compensation method, the V_{TH} is compensated by six or more TFTs in real time [7], [8]. Although it is a simple method to compensate for V_{TH}, poor compensation performance for low gray levels and the reduced aperture ratio due to too many TFTs are unavoidable. On the other hand, in the case of external compensation, the V_{TH} shift can be compensated by the external circuit [9]–[14]. This method requires fewer TFTs. Thus, the aperture ratio can be increased, contributing to the display with ultra-high resolution.

In addition to its excellent performance as a display, multifunctional micro-LEDs with various functions such as temperature sensing, light energy harvesting, and light detection are being studied [15]. Because the reverse-current through an LED is affected by the incident light, micro-LEDs can be utilized as photodetectors to sense the intensity of incident lights. Thus, micro-LEDs can be used as fingerprint sensors as well as display devices. The fingerprint recognition has been employed as a method to enhance device security [16], [17]. A fingerprint is a pattern composed of ridges and valleys, which are represented by the convex and concave regions of a fingertip, respectively. Many researchers have investigated various fingerprint recognition methods in display systems, such as ultrasonic, capacitive, and optical methods [17]–[22]. All of the technologies, however, need additional sensors to recognize fingerprints. In addition, the user must touch a pre-determined small area where the sensors are attached.

In this study, we propose a new micro-LED display architecture that features fingerprint recognition without additional sensors and the external compensation method for ultra-high resolutions.

II. Proposed Pixel Circuit

Fig. 1 shows I-V characteristics of a red LED in reverse bias. The colored solid lines in Fig. 1 show the I-V characteristics of the red LED under various irradiance. The black dashed line represents the I-V characteristics without any incident light. The I-V characteristics of the red LED were measured when constant current flowed through a green LED placed 4 mm apart facing each other. The spectral radiance of the green LED depending on current was measured using spectroradiometer and irradiance was calculated. The inset of Fig.1 shows the reverse currents of the red LED depending on irradiance from the green LED when the reverse bias of the red LED was −3 V. The capacitance of LED (C_{LED}) was 30 pF, and the size was 200 μm × 100 μm. Due to the photoelectric effect of LEDs, the LED photocurrents are affected by ambient lights as shown in Fig. 1. Table I shows

Manuscript received 20 June 2022; accepted 1 July 2022. Date of publication 7 July 2022; date of current version 26 August 2022. This work was supported in part by the Technology Innovation Program, On-Panel Circuit Integration and Driving System Technology for 1270 ppi Low-Power OLED Display Based on Oxide Semiconductor through the Ministry of Trade, Industry and Energy (MOTIE), South Korea, under Grant 20016317; and in part by the Brain Korea 21 (BK21) Fostering Outstanding Universities for Research (FOUR) through the Ministry of Education (MOE), South Korea. The review of this letter was arranged by Editor Z. Ma. *(Corresponding author: Seung-Woo Lee.)*

The authors are with the Department of Information Display, Kyung-Hee University, Seoul 02447, South Korea (e-mail: seungwoolee@khu.ac.kr).

Color versions of one or more figures in this letter are available at https://doi.org/10.1109/LED.2022.3189211.

Digital Object Identifier 10.1109/LED.2022.3189211

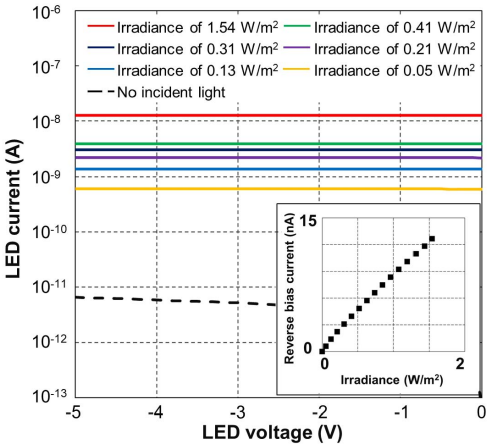

Fig. 1. Measured I-V characteristics and reverse current (inset figure) of a red LED depending on irradiance caused by a green LED.

TABLE I
RESPONSIVITY DEPENDING ON COLORS OF THE LEDS

Responsivity (nA/W/m²)		Emitting LED		
		Red	Green	Blue
Sensing LED	Red	9.2	7.5	2.5
	Green	0.0	0.1	4.4
	Blue	0.0	0.0	0.5

the responsivity depending on the color of the emitting and sensing LEDs. We used green LEDs as emitters and red LEDs as sensors because they showed the highest photocurrent and high responsivity.

We propose a new pixel circuit for a micro-LED display adopting the external compensation method and featuring fingerprint recognition as shown in Fig. 2(a). The proposed circuit comprises four transistors and one capacitor (4T1C) whereas the conventional external compensation circuit is composed of 3T1C [13], [14]. When a finger is placed on the display screen, the pixels under the finger don't need to emit light related to image data. They can be used as light sources or photosensors for fingerprint recognition because the finger blocks lights from LEDs. The intensity of the reflected light is dependent on where it is reflected in the fingerprint (valley or ridge) [6]. In our proposed method, the LEDs under the finger are used as light sources or photosensors. As the light sources, the LEDs emit lights irradiating the finger. As the photosensors, the LEDs generate photocurrents depending on the intensity of the reflected lights from the finger. The generated photocurrents are integrated in the proposed pixel circuit. The right figure of Fig. 2(a) shows the fabricated circuit using oxide TFTs. The channel length of all TFTs was 3 μm. The widths of the driving transistor M_2 and the switching transistor M_1 were 60 μm and 10 μm, respectively. The width of two switching transistors M_3 and M_4 to initialize the anode of the LED was 20 μm, and the storage capacitor was 500 fF. In the experiment, V_{DD}, V_{SS}, and V_1were 5, 0, and −3, respectively. The voltage range of control signals Scan[n], Sense[n], and EM[n] were -7 to 7 V. The conventional external compensation method [13], [14] was applied. When detecting V_{TH}, M_1 keeps on to maintain the V_G. M_3 turns on to initialize the V_S[n]. After Sense[n] becomes low, the drain current flows through M_2. Because of the current, the V_S[n] is charged from

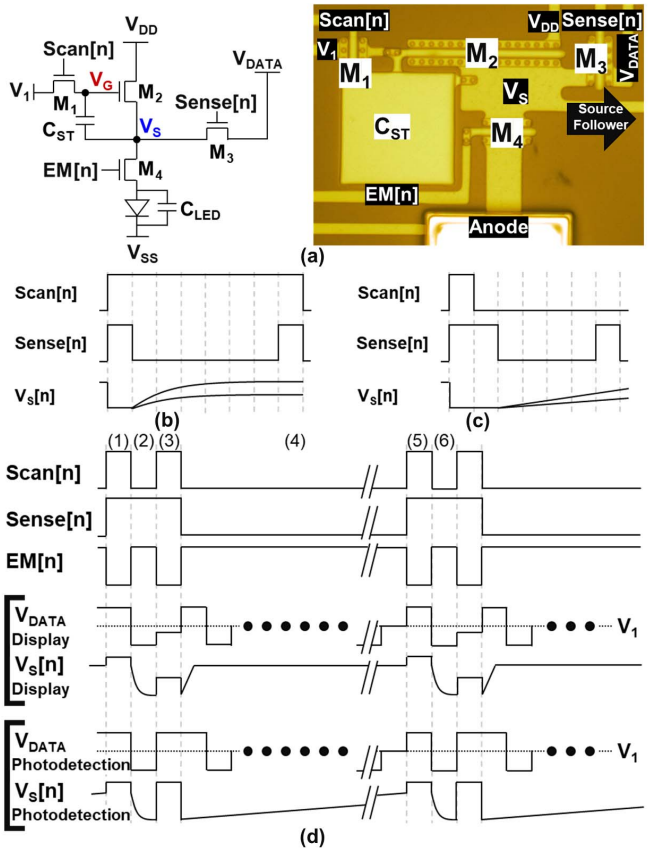

Fig. 2. (a) Proposed circuit diagram and photograph of manufactured pixel circuit and timing diagram of the (b) V_{TH} detection, (c) k detection, and (d) proposed pixel circuit.

the initialized voltage to the voltage where $V_S[n] = V_G$-V_{TH} as shown in Fig. 2(b). V_S[n] does not increase any more if V_S[n] reaches V_G-V_{TH} that means M_2 is off. The k detection can be done after V_{TH} detection. M_1 and M_3 turn on to set V_{GS} of the M_2. At this moment, the V_{GS} includes threshold compensation data. Sense[n] turns off later than Scan[n] to initialize V_S[n], then, V_S[n] increases at a fixed V_{GS} as shown in Fig. 2(c). By measuring the ΔV_S[n] at a given time, we can estimate k of the M_2.

Fig. 2(d) shows the timing diagram for the proposed pixel circuit. One-line time is divided into three periods: V_{GS} reset, anode initialization, and V_{GS} programming. During V_{GS} reset (period (1)), Scan[n] and Sense[n] turn on M_1 and M_3. The gate voltage of M_2 becomes V_1. M_2 is turned off because V_S becomes higher than V_1. In the anode initialization (period (2)), Scan[n] goes low and EM[n] goes high. Sense[n] keeps high, so the anode voltage of LED is initialized by M_3 and M_4 while keeping the M_2 off. In display operation, during the V_{GS} programming (period (3)), Scan[n] and Sense[n] are high, and EM[n] goes low. V_{DATA} becomes image data voltage including V_{TH} compensation. Then, V_{GS} of M_2 can be set according to the image data. The source node voltage V_S[n] abruptly drops down at the beginning of period (4) because C_{LED} is far higher than parasitic capacitance at the source node. But V_S[n] goes up so that the LED current matches what the V_{GS} of M_2 determines. In photo-detecting operation, during V_{GS} programming (period (3)), the V_{GS} that turns off the M_2 is set. Thus, there is no current from M_2 even when M_4 turns on. Then, the source node voltage rises depending

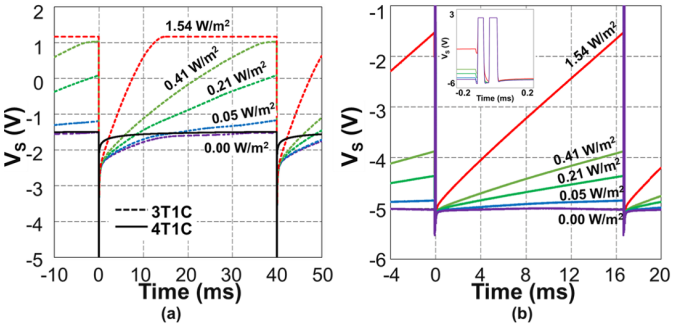

Fig. 3. (a) Comparison of measured V_S in 3T1C (dashed lines) and 4T1C (solid lines) pixel circuits and (b) the charge integration performance of the proposed 4T1C circuit depending on irradiance.

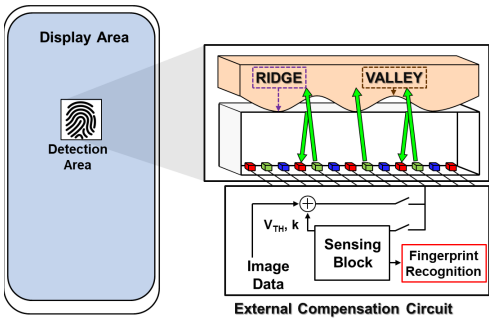

Fig. 4. Proposed novel display architecture featuring fingerprint detection.

on the LED photocurrent caused by the lights reflected from the interface between the fingerprint and the cover glass. The accumulated charges caused by the photocurrent are read through V_{DATA} line by using a charge amplifier in the driver IC in period (6). $V_S[n]$ becomes the voltage for V_{GS} reset during period (5). However, in the beginning of the period (6), $V_S[n]$ becomes almost the same as the final anode voltage (V_{FA}) in period (4) because one node of CST becomes floated and C_{LED} is very large. Thus, it is possible to read the accumulated charges during period (6). In this way, the proposed circuit can perform fingerprint recognition.

III. Experimental Results and Discussion

Fig. 3(a) shows the measured V_S when V_{TH} detection method was applied. The dashed and solid lines indicate the measured V_S depending on irradiance in 3T1C and 4T1C pixel circuits, respectively. At the beginning of V_{TH} detection, the currents of M_2 with V_{GS} of 2 V dominated the voltage increase. So, the V_S of −5 V rapidly increases to the voltage where $V_S = V_G$-V_{TH}. When V_S increased to V_G-V_{TH}, M_2 was turned off, but photocurrent of LED was still present. Thus, the V_S was increased with a higher voltage regardless of V_{TH} of M_2.

The larger the irradiance, the more photocurrent flowed and the larger the voltage changed. Measured V_S at 40 ms were −1.51, −1.17, 0.10, 1.03, and 1.17 V, where the irradiances were 0.00, 0.05, 0.21, 0.41, and 1.54 W/m^2, respectively. Because the gate voltage of M_2 was −3 V, estimated V_{TH} were −1.50, −1.83, −3.10, −4.03, and −4.17 V, which means that V_{TH} compensation is impossible.

The black solid line in Fig. 3(a) shows the measured V_S in 4T1C circuit depending on irradiance. A voltage of −7 V was applied to the gate of M_4. The measured V_S was the same regardless of irradiance as shown in Fig. 3(a), which means that the proposed 4T1C circuit can compensate for V_{TH} regardless of the ambient lights.

Generally, V_{TH} detection of external compensation is done when the display is turned off because it takes a long time. During the procedure, the ambient light may change dynamically, and the corresponding effects are uncontrollable. Furthermore, Ambient lights with a broader spectrum will increase the V_S faster. Therefore, M_4 that blocks the harmful effects of LED is indispensable in the pixel circuit adopting the external compensation for AM micro-LED displays.

Fig. 3(b) shows the measured V_S depending on irradiance when the LED was used as a photosensor. The inset figure in Fig. 3(b) is an enlarged view of the same waveform between −0.2 to 0.2 ms. To turn off the M_2, 2 V was applied during the periods (1) and (3). −5 V was applied during period (2) to initialize the anode as shown in the inset figure. V_S measured after one frame time (16.7 ms) reached −5.02, −4.84, −4.36, −3.88, and −1.53 V under the irradiance of 0.00, 0.05, 0.21, 0.41, and 1.54 W/m^2.

Optical fingerprint recognition methods distinguish the intensity of reflected lights caused by refractive index difference. The light intensity reflected at the valley of the fingerprint is about 33 times stronger than that reflected at the ridge. Due to the linearity between the irradiance and the photocurrent as shown in Fig. 1, the photocurrents according to the pattern of the fingerprint will also be different by 33 times. The irradiance of 1.54 W/m^2 is 30 times higher than 0.05 W/m^2. The final readout voltages were −5.02 V and −1.53 V for 0.05 and 1.54 W/m^2, respectively. This big readout voltage difference of 3.49 V implies that the proposed AM micro-LED display will easily distinguish the ridges and valleys of fingerprints.

The proposed driving architecture is depicted in Fig. 4. Built-in touch sensors provide information on where the fingertip is located. The LED pixels under the fingertip act as light sources or photosensors for the optical fingerprint recognition. The LED pixels outside the fingertip emit lights to display an image. Thus, fingerprint recognition is possible everywhere because all the LED pixel circuits are the same structure. There are no side-effects caused by additional light sources and sensors. The external compensation technology requires the sensing capability of the source driver IC. By measuring the source node voltage of the driving transistor, V_{TH} and mobility are sensed and a compensated data voltage is applied. Our proposed method also reads accumulated charges through source nodes of driving transistors. Thus, both fingerprint recognition and external compensation are possible if our simple 4T1C architecture without additional sensors is adopted.

IV. Conclusion

A new AM micro-LED display architecture adopting external compensation that enables fingerprint recognition without any additional light sources and sensors has been proposed. A fingerprint can be recognized anywhere because all the LED pixel circuits are the same structure. Furthermore, multiple fingerprints are also recognized, which can strengthen the security of mobile devices with the AM micro-LED display adopting our proposed architecture.

REFERENCES

[1] Z. Chen, S. Yan, and C. Danesh, "MicroLED technologies and applications: Characteristics, fabrication, progress, and challenges," *J. Phys. D, Appl. Phys.*, vol. 54, no. 12, Jan. 2021, Art. no. 123001, doi: 10.1088/1361-6463/abcfe4.

[2] Y. Huang, E.-L. Hsiang, M.-Y. Deng, and S.-T. Wu, "Mini-LED, micro-LED and OLED displays: Present status and future perspectives," *Light, Sci. Appl.*, vol. 9, no. 1, Jun. 2020, Art. no. 105, doi: 10.1038/s41377-020-0341-9.

[3] T. Wu, C.-W. Sher, Y. Lin, C.-F. Lee, S. Liang, Y. Lu, S.-W. Huang Chen, W. Guo, H.-C. Kuo, and Z. Chen, "Mini-LED and micro-LED: Promising candidates for the next generation display technology," *Appl. Sci.*, vol. 8, no. 9, p. 1557, Sep. 2018, doi: 10.3390/app8091557.

[4] W.-J. Wu, L. Zhou, M. Xu, L.-R. Zhang, R.-H. Yao, and J.-B. Peng, "An AC driving pixel circuit compensating for TFTs threshold-voltage shift and OLED degradation for AMOLED," *J. Display Technol.*, vol. 9, no. 7, pp. 572–576, Mar. 2013, doi: 10.1109/JDT.2013.2250254.

[5] K.-Y. Lee and P. C.-P. Chao, "A new AMOLED pixel circuit with pulsed drive and reverse bias to alleviate OLED degradation," *IEEE Trans. Electron Devices*, vol. 59, no. 4, pp. 1123–1130, Apr. 2012, doi: 10.1109/TED.2012.2184289.

[6] G. R. Chaji, S. Alexander, J. M. Dionne, Y. Azizi, C. Church, J. Hamer, J. Spindler, and A. Nathan, "Stable RGBW AMOLED display with OLED degradation compensation using electrical feedback," in *IEEE Int. Solid-State Circuits Conf. (ISSCC) Dig. Tech. Papers*, Feb. 2010, pp. 118–119, doi: 10.1109/ISSCC.2010.5434027.

[7] J.-P. Lee, H.-S. Jeon, D.-S. Moon, and B. S. Bae, "Threshold voltage and IR drop compensation of an AMOLED pixel circuit without a V_{DD} line," *IEEE J. Electron Devices Soc.*, vol. 35, no. 1, pp. 72–74, Jan. 2014, doi: 10.1109/LED.2013.2289315.

[8] Y. H. Jang, D. H. Kim, W. Choi, M.-G. Kang, K. I. Chun, J. Jeon, Y. Ko, U. Choi, S. M. Lee, J. U. Bae, K.-S. Park, S. Y. Yoon, and I. B. Kang, "*7–4: Invited paper*: Internal compensation type OLED display using high mobility oxide TFT," in *SID Symp. Dig. Tech. Papers*, vol. 48, 2017, pp. 76–79, doi: 10.1002/sdtp.11567.

[9] K.-S. Kang, J.-K. Lee, J.-M. Kang, and S.-Y. Lee, "A novel real-time TFT threshold voltage compensation method for AM-OLED using double sampling of source node voltage," *IEEE J. Electron Devices Soc.*, vol. 9, pp. 311–317, 2021, doi: 10.1109/JEDS.2021.3058348.

[10] H.-J. Shin, S. Takasugi, K.-M. Park, S.-H. Choi, Y.-S. Jeong, B.-C. Song, H.-S. Kim, C.-H. Oh, and B.-C. Ahn, "7.1: *Invited paper*: Novel OLED display technologies for large-size UHD OLED TVs," in *SID Symp. Dig. Tech. Papers*, vol. 46, 2015, pp. 53–56, doi: 10.1002/sdtp.10225.

[11] H.-J. Shin, S. Takasugi, K.-M. Park, S.-H. Choi, Y.-S. Jeong, H.-S. Kim, C.-H. Oh, and B.-C. Ahn, "50.1: *Invited paper*: Technological progress of panel design and compensation methods for large-size UHD OLED TVs," in *SID Symp. Dig. Tech. Papers*, vol. 45, Jul. 2014, pp. 720–723, doi: 10.1002/j.2168-0159.2014.tb00189.x.

[12] S. Mizukoshi, "Organic light emitting diode display device for pixel current sensing and pixel current sensing method thereof," U.S. Patent 20130050292 A1, Feb. 28, 2013. [Online]. Available: https://patents.google.com/patent/US20130050292A1/en

[13] R. Tani, J.-S. Yoon, S.-I. Yun, W.-J. Nam, S. Takasugi, J.-M. Kim, J.-K. Park, S.-Y. Kwon, P.-Y. Kim, C.-H. Oh, and B.-C. Ahn, "64.2: Panel and circuit designs for the world's first 65-inch UHD OLED TV," in *SID Symp. Dig. Tech. Papers*, vol. 46, 2015, pp. 950–953, doi: 10.1002/sdtp.10423.

[14] Y.-F. Jin and H.-J. Xie, "P-1.8: External compensation for TFT Vth&mobility using linear charge sense method in AMOLED display," in *SID Symp. Dig.*, vol. 49, Apr. 2018, pp. 541–543, doi: 10.1002/sdtp.12776.

[15] Z. Liu, K. Zhang, Y. Liu, S. Yan, H. S. Kwok, J. Deen, and X. Sun, "Fully multi-functional GaN-based micro-LEDs for 2500 PPI micro-displays, temperature sensing, light energy harvesting, and light detection," in *IEDM Tech. Dig.*, Dec. 2018, pp. 38.1.1–38.1.4, doi: 10.1109/IEDM.2018.8614692.

[16] W. Yang, S. Wang, J. Hu, G. Zheng, and C. Valli, "Security and accuracy of fingerprint-based biometrics: A review," *Symmetry*, vol. 11, no. 2, p. 141, Jan. 2019, doi: 10.3390/sym11020141.

[17] S. Memon, M. Sepasian, and W. Balachandran, "Review of finger print sensing technologies," in *Proc. IEEE Int. Multitopic Conf.*, Karachi, Pakistan, Dec. 2008, pp. 226–231, doi: 10.1109/INMIC.2008.4777740.

[18] T. Shimamura, H. Morimura, S. Shigematsu, M. Nakanishi, and K. Machida, "Capacitive-sensing circuit technique for image quality improvement on fingerprint sensor LSIs," *IEEE J. Solid-State Circuits*, vol. 45, no. 5, pp. 1080–1087, May 2010, doi: 10.1109/JSSC.2010.2042525.

[19] F. Alonso-Fernandez, F. Roli, G. L. Marcialis, J. Fierrez, and J. Ortega-Garcia, "Comparison of fingerprint quality measures using an optical and a capacitive sensor," in *Proc. BTAS*, Crystal City, VA, USA, Sep. 2007, pp. 1–6, doi: 10.1109/BTAS.2007.4401956.

[20] S.-W. Back, Y.-G. Lee, S.-S. Lee, and G.-S. Son, "Moisture-insensitive optical fingerprint scanner based on polarization resolved in-finger scattered light," *Opt. Exp.*, vol. 24, no. 17, pp. 19195–19202, Aug. 2016, doi: 10.1364/OE.24.019195.

[21] T. Kamada, R. Hatsumi, K. Watanabe, S. Kawashima, M. Katayama, H. Adachi, T. Ishitani, K. Kusunoki, D. Kubota, and S. Yamazaki, "OLED display incorporating organic photodiodes for fingerprint imaging," *J. Soc. Inf. Display*, vol. 27, no. 6, pp. 361–371, Apr. 2019, doi: 10.1002/jsid.786.

[22] W.-J. Peng, Y.-C. Cheng, J.-S. Lin, M.-F. Chen, and W.-S. Sun, "Development of miniature wide-angle lens for in-display fingerprint recognition," *Proc. SPIE*, vol. 11231, pp. 38–44, Feb. 2020, doi: 10.1117/12.2545463.